THE JOURNAL OF PHYSICAL CHEMISTRY Letters

Perspective

pubs.acs.org/JPCL

Toward Ending the Guessing Game: Study of the Formation of Nanostructures Using In Situ Liquid Transmission Electron Microscopy

Thao Ngo and Hong Yang*

Department of Chemical and Biomolecular Engineering, University of Illinois at Urbana−Champaign, 206 Roger Adams Laboratory, Box C-3, MC-712, 600 South Mathews Avenue, Urbana, Illinois 61801, United States

ABSTRACT: The field of synthetic nanochemistry has grown tremendously in the past three decades since the discovery of nonaqueous synthesis of monodispersed particles. Almost all classes of materials, from II−VI semiconductor to metal, alloy, and metal oxide can now be prepared in various sizes and shapes. One major challenge has been the development of a technique for direct real-time recording of data during the formation of nanostructures in liquid reaction media where nucleation and growth occur. A viable solution finally arrived with the recent development of static and flow liquid cells for transmission electron microscopy (TEM). This Perspective will showcase a few selected examples in this rapidly growing area, with a focus on using the new capabilities of liquid TEM (LTEM) for quantitative study of nucleation and growth, as well as shape formation of nanocrystals in solution. A discussion on future direction is also presented.

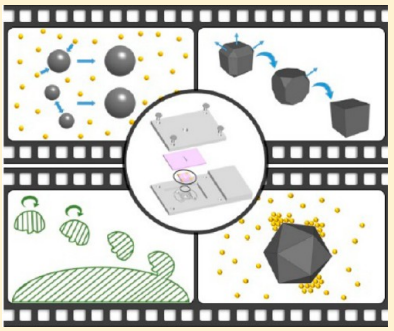

The invention of transmission electron microscopy (TEM) has led to major advancements in many research fields, including the nucleation and growth of nanoparticles.[1] In many studies on the formation mechanism, a glimpse into growth stages is acquired with TEM micrographs taken with specimen of nanoparticles made postsynthetically.[2−4] Such ex situ technique, however, cannot help to understand the details of the dynamic process of nucleation and growth in solution, and there is a need to bridge the gap between what happens in real time and what is observed in postsynthesis imaging. The idea of using a closed chamber to image liquid-suspended samples in TEM is so appealing that the initial concept was conceived five years after the invention of TEM.[5] Two years later, a closed chamber was made using two Pt discs with a colloid film as window materials and sealed by rings of adhesive.[6]

Fast forward to 2003, a practical, functional liquid cell was finally introduced for use in TEM. The key advancement was the use of ultrathin silicon nitride (SiN) substrate as window material, which is capable of withstanding ultrahigh vacuum.[7] In the early design, the liquid cell used silicon (Si) wafers, which were glued face-to-face and sealed from vacuum by an O-ring, as the supporting substrate. The top and bottom of Si pieces were deposited with electronically transparent SiN films as the windows as shown in Figure 1a. The liquid cell was used to investigate the electrochemical growth of copper nanoclusters at the solid−liquid interface in a TEM at a rate of 30 images/s and a spatial resolution of 5 nm.[7] Direct observation of nanoparticle growth in real time and in a liquid environment thus became possible.

The liquid cell has since been utilized in a number of research areas, including crystal growth, mineralization,[8,9] lithium battery,[10,11] and life sciences.[12−15] Study on the formation of nanocrystals in particular has benefitted from this new technology.[16−21] In one popular design, a liquid mixture is introduced between two SiN windows. The cell is placed in the tip region of the sample holder using vacuum-tight O-rings, as shown in Figure 1b. Recent innovations of liquid cell technology also include the use of graphene as novel window materials to bring the resolution to the atomic level (Figure 1c),[15,20] the introduction of microchannels to allow the flow of liquid,[22] and electrical biasing for electrochemical study (Figure 1d).[7]

For years the nucleation and growth of nanoparticles have been described by the theories developed by LaMer, Ostwald, and others.[23,24] In all these frameworks, the process is described as an intertwined, three-staged process involving rapid increase in the concentration of precursors until a critical concentration is achieved, reduction in the concentration of free monomers due to the burst nucleation, and the growth influenced by the diffusion of precursors from solution to nuclei, surface deposition, and ripening. Such nucleation and growth theory is often illustrated by the LaMer diagram, which depicts the concentration of solutes as a function of time,[23] and is modeled by the Lifshitz−Slyozov−Wagner (LSW) theory, which takes both diffusion and reaction into consideration.[25,26]

Recent innovation in using in situ liquid cell technology in studying the formation of nanoparticles offers a new direct method to verify existing theories and, in many cases, uncover complex processes that were once thought to follow different pathways. For example, Zheng et al. showed that nuclei

Received: October 4, 2015
Accepted: November 24, 2015
Published: November 24, 2015

DOI: 10.1021/acs.jpclett.5b02210
J. Phys. Chem. Lett. 2015, 6, 5051−5061

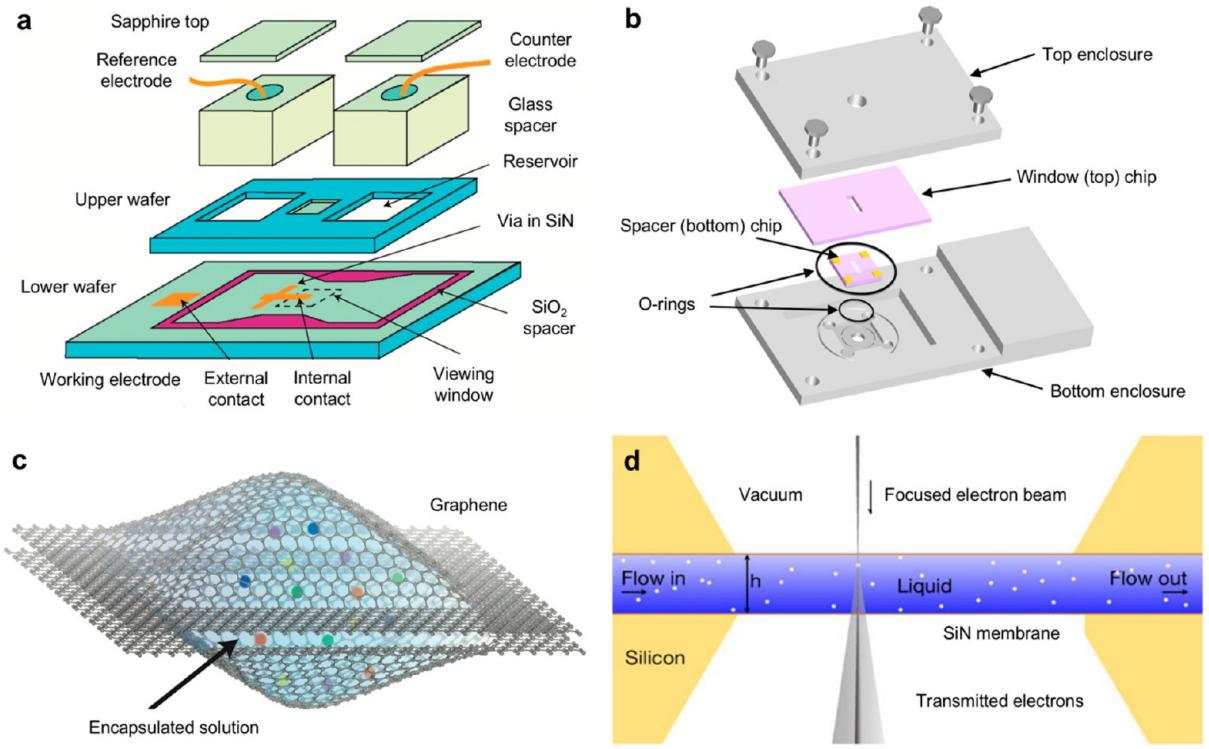

Figure 1. Illustration of different types of liquid cells. (a) Components of an early design of a liquid cell with electrical biasing capability. Image is adapted with permission from ref 7. Copyright 2003 Nature Publishing Group. (b) Components of a liquid static cell. (c) Liquid graphene cell. Image is reprinted with permission from ref 20. Copyright 2012 American Association for the Advancement of Science. (d) Cross section of liquid flow cell. Image is reprinted with permission from ref 13. Copyright 2011 Nature Publishing Group.

Recent innovation in using in situ liquid cell technology in studying the formation of nanoparticles offers a new direct method to verify existing theories and, in many cases, uncover complex processes that were once thought to follow different pathways.

underwent monomer addition and coalescence simultaneously. In the later process, particles relaxed and rearranged, reaching to the sizes similar to those formed via addition of monomers.[16] Details of oriented attachment, in which two Pt nanoparticles rotated to a preferred orientation and then coalesced, were also observed in situ.[27] Yang and Zuo groups recently showed that deposition of Au on icosahedral Pt nanoparticles is a much more complex process than those for two-dimensional (2D) heterogeneous nucleation and growth, involving initial process at corners, followed by surface diffusion and finally layer-by-layer growth.[28] In this paper, these studies, along with other significant advancements in nucleation and growth using LTEM, will be discussed. We hope to show readers how LTEM has propelled the understanding of nucleation and growth of nanoparticles to a more quantitative level than ever before. This Perspective will focus on recent work in the following three main areas: (1) liquid static cells, including the graphene cell, (2) liquid flow cells, and (3) the use of electrons from the beam to study the formation of nanoparticles. We close with remarks on the current state and outlooks of this promising field.

In Situ LTEM Study of the Formation of Nanostructures in Static Environment. In a typical experiment, solution mixture or liquid suspension is placed on top of a chip or drawn into a liquid cell by capillary force during assembly. Using such a static cell, the formation of colloidal Pt nanocrystals was revealed to follow two competing processes: addition of monomers and coalescence of small particles, as shown in Figure 2a.[16] Moreover, the particles formed via coalescence were found to undergo a period of structural relaxation, called punctuated growth, wherein monomers continued to add to the other particles. The relaxation time, τ, followed a power law relationship with the size in diameter of nanoparticle, that is, τ is proportional to $d^{3.3}$, where d is diameter. After the relaxation, particles resumed the growth via addition of precursors. The quantitative analysis showed a jump in size after each coalescence event, resulting in a particle with a larger average size from a bimodal distribution through size focusing (Figure 2a). Multiple coalescence mainly contributed to the size focusing and was common among small particles due to their high surface energy and mobility, and thus high collision rate. This study shows the size focusing of nanocrystals through punctuated growth correlated with coalescence. This feature has not been taken into consideration in the classical models for nanocrystal growth, demonstrating the remarkable capability of LTEM in direct visualization of missing details in the nucleation and growth process.

In addition to SiN, graphene is another excellent material in keeping liquid samples sealed under vacuum for LTEM study because of its several unique properties. First, graphene has excellent electron transparency due to its single-carbon-layer

DOI: 10.1021/acs.jpclett.5b02210
J. Phys. Chem. Lett. 2015, 6, 5051−5061

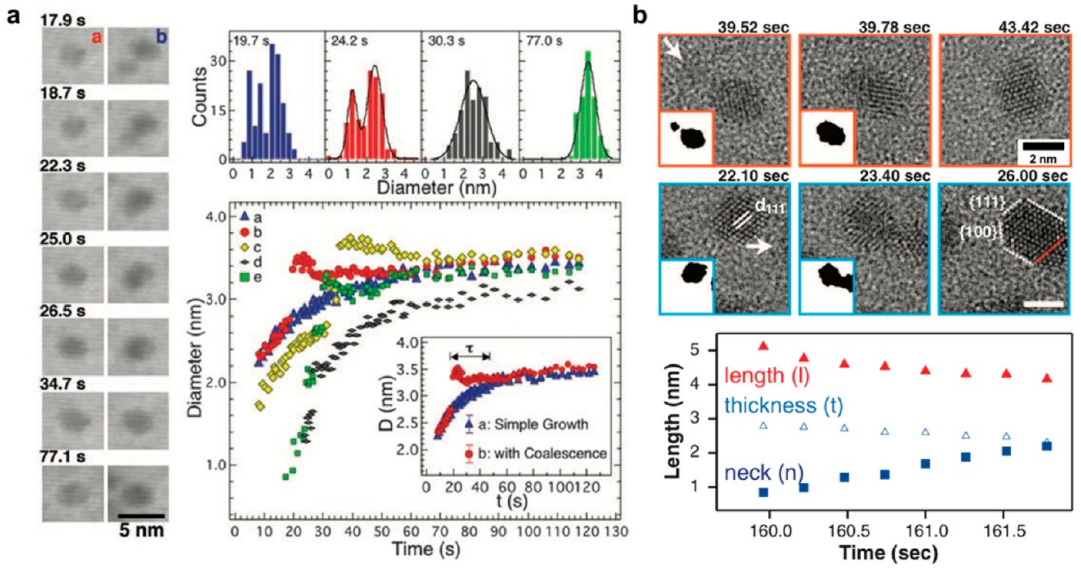

Figure 2. Quantitative analyses of nucleation and growth kinetics of nanoparticles. (a) Growth of colloidal Pt nanocrystals via monomer addition and coalescence. Image is adapted with permission from ref 16. Copyright 2009 American Association for the Advancement of Science. (b) Growth of colloidal Pt nanocrystals in a graphene liquid cell. Image is adapted with permission from ref 20. Copyright 2012 American Association for the Advancement of Science.

thickness.[29] Second, carbon atoms pack closely, making graphene highly impermeable even to helium atoms.[30] Third, the graphene sheet is highly flexible and can tightly wrap around a liquid droplet.[31] Fourth, graphene can withstand large difference in pressure between the inside and outside of a liquid cell in a TEM chamber.[31] Finally, buildup of electrostatic charge can be reduced because graphene has good electrical conductivity.[32] Similarly, heat generated due to the irradiation of electron beam can be dissipated efficiently because of the good thermal conductivity.[33]

Graphene liquid cell (GLC) was made by encapsulating a solution between two pieces of graphene.[20] Site-selective coalescence, structural reconstruction, and other phenomena were examined by GLC. Both monomer addition and multiple coalescence of Pt nanocrystals were observed using such graphene cells (Figure 2b). The use of GLC also enables direct visualization of important details of the coalescence, such as the requirement for specific nanocrystal orientation. The nanoparticles were seen to coalesce at {111} planes through joining either two identical planes to form a single crystal or mirror planes for a twin crystal. The Pt nanoparticles preferred to coalesce at the {111} planes of an fcc phase crystal, because they have the lowest surface energy and are expected to have a low coverage by ligands. Thus, metal nanocrystals that come in contact on the {111} planes are able to coalesce, because they experience minimal obstruction due to surface capping. Another important observation was the correlated motion of two nanocrystals from about 100 s prior to coalescence, which aided in alignment to match the lattices. As the Pt nanoparticles approached one another, the center-to-center distance fluctuated between 4 to 6 nm for 26 s. The nanoparticles rolled and slid over each other until the lattice aligned, and then they coalesced. The GLC not only helped to confirm the growth trajectories but also provided new details because it offered high-resolution in situ images of liquid samples.

LTEM has also helped to identify a new method to reverse particle coarsening via Ostwald ripening, in which small particles dissolve and redeposit onto large particles to reduce the overall surface energy.[21] Alternating growth and dissolution of bismuth (Bi) nanocrystals was achieved by creating a precursor-scarce environment in a liquid cell. The precursor-scarce solution was created by adding a limited number of large Bi nanoparticles in a mixture of oleylamine and dicholorobenzene into the liquid cell. As the temperature rose to 180 °C, the Bi nanoparticles started to dissolve to generate precursors in the solution. The Bi precursors then diffused to the surrounding area and nucleated to form new Bi nanoparticles. Nearly all nanoparticles experienced an oscillation of growth and dissolution, which was accomplished via the exchange of precursors between nanoparticles through their local environment. By tracking the volume change of nanoparticles along their growth trajectories, the growth rate was established to be inversely dependent on particle size, that is, dr/dt was proportional to $1/r$. The dissolution rate, however, was more complex as it was not a simple function of particle size. The presence of a depletion zone around a nanoparticle, resulting from small clusters in a diffusion layer being consumed by large, stable clusters, was evidenced by the direct observation of change in the pairwise correlation coefficient as the distance between two particles decreased. This depletion zone often plays an important role in the mass transport between a pair of nanoparticles going though oscillatory growth. As a particle grew, it consumed precursors in the surrounding environment. The dynamics between the deposition of precursors and dissolution of particles resulted in an oscillatory growth. The coarsening of nanoparticles via Ostwald ripening often results in a loss of active surface area, an important reason for the decreased catalytic activity over time. Thus, in situ results should help to develop a strategy on making stable and durable nanocatalysts by preventing coarsening due to Ostwald ripening.

LTEM study allows to uncover new insight on the coalescence of nanoparticles in solution through oriented attachment, wherein particles in close proximity spontaneously rotate and align at proper crystalline surfaces prior to the attachment.[34] Precise control of oriented attachment is

DOI: 10.1021/acs.jpclett.5b02210
J. Phys. Chem. Lett. 2015, 6, 5051−5061

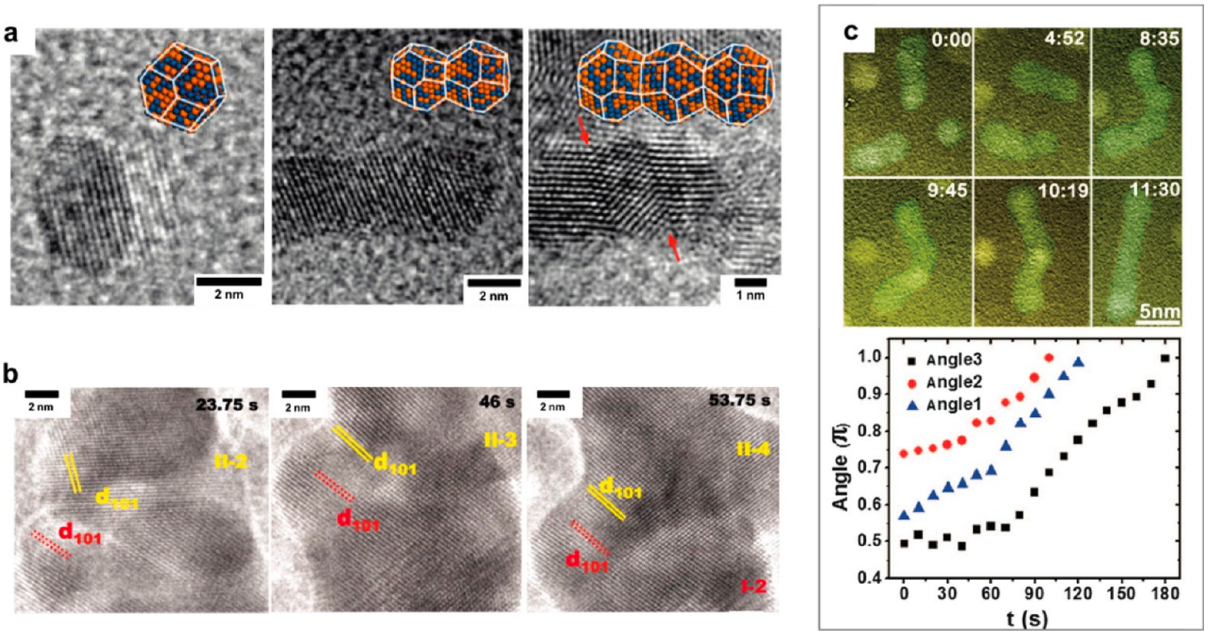

Figure 3. (a) Ex situ TEM study on the growth of PtAg nanowires. Image is adapted with permission from ref 3. Copyright 2010 American Chemical Society. (b) LTEM images showing the rotation of two nanoparticles of iron oxyhydroxide in oriented attachment. Image is adapted with permission from ref 27. Copyright 2012 American Association for the Advancement of Science. (c) In situ LTEM study of growth of Pt_3Fe nanowires using a liquid static cell. Image is adapted with permission from ref 43. Copyright 2012 American Association for the Advancement of Science.

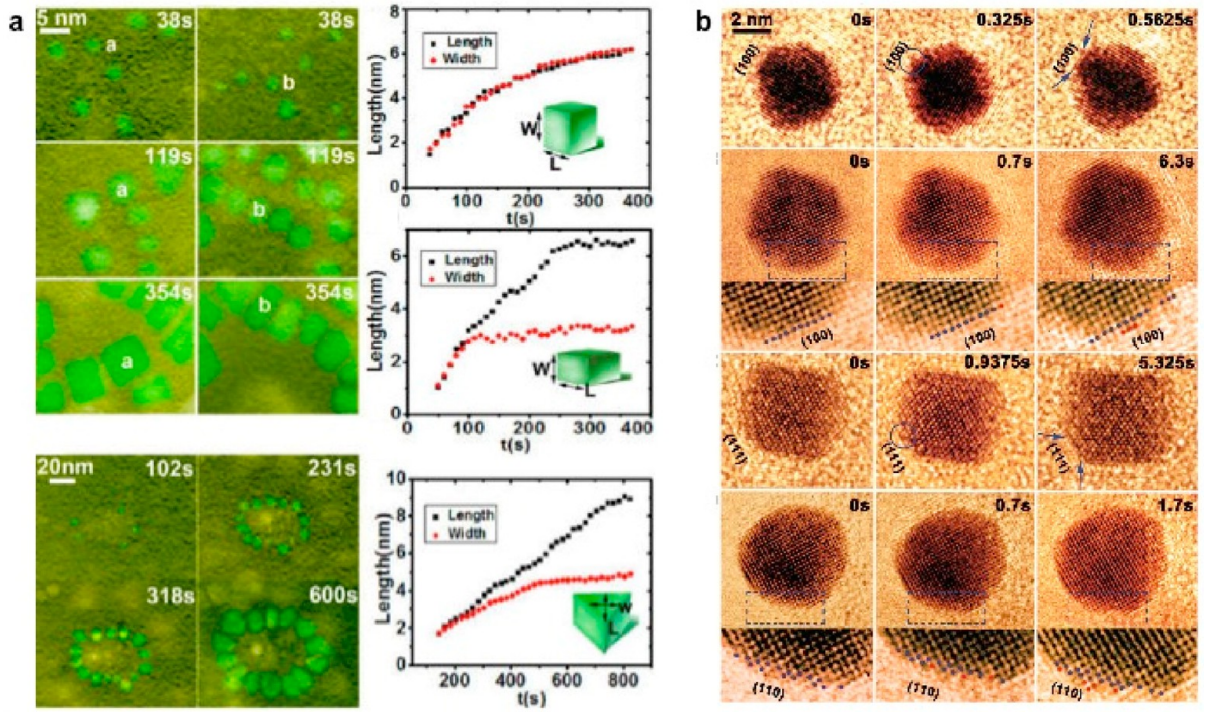

Figure 4. In situ LTEM study of the development of facets using liquid static cell. (a) Shape development of Pt−Fe nanoparticles. Image is reprinted with permission from ref 46. Copyright 2013 American Chemical Society. (b) Formation of the facets during the growth of Pt nanocubes. Image is adapted with permission from ref 17. Copyright 2014 American Association for the Advancement of Science.

potentially useful in the generation of interesting anisotropic nanostructures.[35] In this context, oriented attachment was studied in the formation of nanostructures of various shapes[36,37] and compositions,[38−42] but the details of the processes for the formation were often missing. One specific example is the formation of platinum−silver (PtAg) nanowires in the presence of oleylamine and oleic acid.[3] Experimental data showed the resulting morphology of alloyed nanostructures was closely related to the composition. Ex situ TEM study and computer simulation results suggest that nanowires grew via attachment on the Ag-rich facets of primary PtAg nanoparticles (Figure 3a).[3] The dynamics of this oriented attachment process, however, remained unclear until recently through a study of the growth of iron oxide-based nanoparticles in a liquid

DOI: 10.1021/acs.jpclett.5b02210
J. Phys. Chem. Lett. 2015, 6, 5051−5061

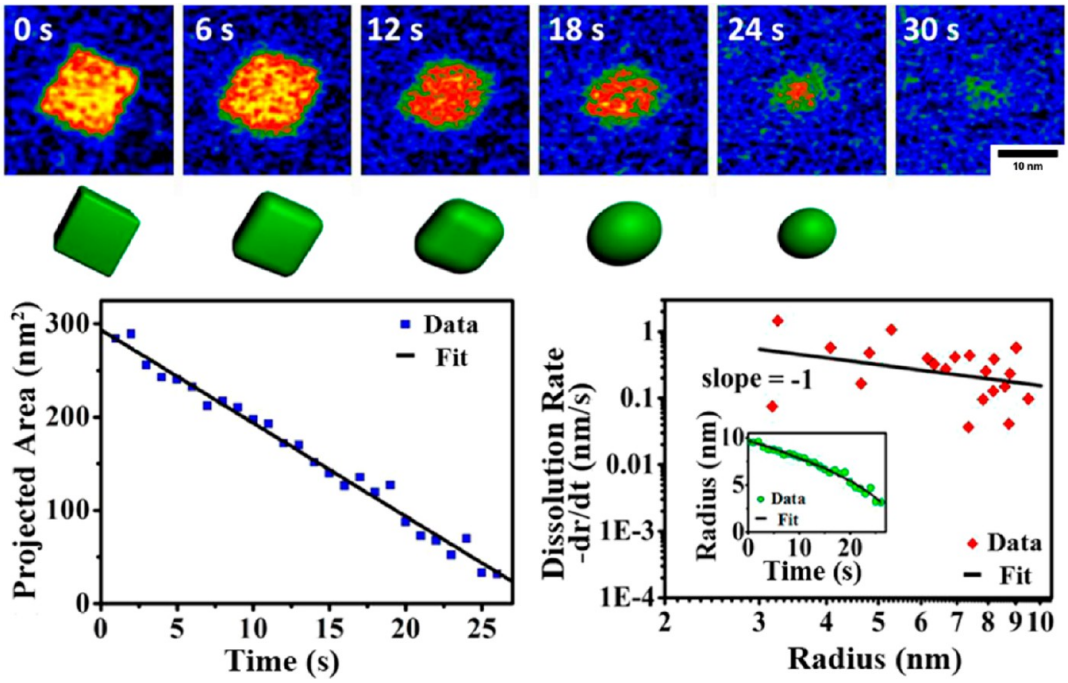

Figure 5. In situ LTEM study of the dissolution of Pd nanocubes using a liquid static cell. Image is reprinted with permission from ref 57. Copyright 2014 American Chemical Society.

cell.[27] Similar to colloidal Pt,[16] iron oxide-based nanoparticles grew via both monomer addition and multiple coalescence events. In situ LTEM revealed repeated contacts and rotations of two particles at nanometer length scale prior to the attachment. Translational and rotational speeds increased as the particles approached one another.[27] When two particles coalesced, they aligned at either the same crystallographic orientation or through the formation of twin. In particular, this in situ study showed two particles misaligned by 54° rotated in opposite directions by +45° and −9°, respectively, resulting in perfect crystallographic alignment (Figure 3b). In this case, oriented attachment was thought to be driven by a short-range force, likely originated from the Coulomb interaction, and was highly sensitive to orientation and affinity at a distance less than 1 nm. Direct observation of the growth of Pt_3Fe nanorod in solution was also achieved (Figure 3c).[43] In situ TEM observation revealed the winding polycrystalline chains formed first via shape-directed attachment before these nanoparticles finally turned into straight single crystalline rods through the following steps. First, nanoparticles formed from monomers and through coalescence, followed by relaxation into spherical shape. Second, these nanoparticles interacted with each other to form chains. Finally, adjacent nanoparticles in the chain contracted to form a neck at which surfactant molecules were excluded. In situ GLC data were used to obtain quantitative velocity profile as a function of distance as a particle approached another particle or a chain. The results showed that a nanoparticle typically moved randomly until it reached a critical distance to another one or chain, at which point it started to drift.[43]

Shape control of faceted nanocrystals such as octahedron and icosahedron is important due to its technological relevance in catalysis and beyond. Despite impressive recent achievements in this area, many questions remain about the formation mechanisms and kinetics, with limited new advancement by theoretical models.[2−4,44,45] In situ LTEM study has offered important clues on the formation of faceted nanostructures. New insights were obtained on the cooperative effect of neighboring nanoparticles on shape evolution of Pt−Fe nanocrystals in oleylamine (Figure 4a).[46] When nanoparticles assembled into a chain, the one in the middle grew into a rectangular shape while those at the end turned into a cube shape. The growth rate along the width direction was identical to that along the length of a nanoparticle at the end of the chain. The nanoparticle in the middle of the chain ceased to grow along the width direction when it was about 1 to 2 nm away from the neighboring nanoparticles. When the nanoparticles assembled into a circle, many turned into trapezoid shape apparently because of the stereo hindrance imposed by neighboring nanoparticles.[46] Clearly, such detailed information on growth and change in morphology could only be achieved with LTEM study in situ in a solution and is too complex to be predicted by theory. A detailed in situ study was also carried out on the facet development of cubic Pt nanocrystals (Figure 4b).[17] The in situ results showed all low index facets grew at similar rates in the presence of oleylamine at the beginning of the process. After the center to surface distance of the crystal reached 2.5 nm, growth of {100} facets stopped, whereas the other low index surfaces such as {110} and {111} continued to develop until {110} facets became confined by two neighboring {100} facets and then stopped. Similarly, growth of {111} facets proceeded until it was halted by three neighboring {100} facets. TEM analysis showed that small clusters of atoms directly attached and propagated on the {100} and {111} facets. The {110} facets however grew with steps as atomic clusters (Figure 4b).[17] Such kinetic analysis offered many details on the formation of facets, which have never been seen before and could play an important role in the future design of nanostructures with desired morphology.

In Situ LTEM Study of Nucleation and Growth of Oxide Nanocrystals from Solutions. LTEM has mainly been used to observe the formation of metal and alloy nanoparticles, but it

DOI: 10.1021/acs.jpclett.5b02210
J. Phys. Chem. Lett. 2015, 6, 5051−5061

was used lately to examine the nucleation of crystals of metal oxides from salt solutions. Nucleation of such systems has been described by several theories including the classical nucleation theory and nonclassical elements such as dense liquid phases[47−49] or metastable clusters.[50] In the cases that involve minerals, it is unclear whether the formation of a final, stable phase is the result of direct nucleation from solution or multistep phase transformation.[51] A recent LTEM study shows both direct and indirect pathways took place simultaneously in the nucleation of calcite crystals ($CaCO_3$).[8] Evidence for the direct nucleation includes the formation of amorphous calcium carbonate (ACC) and vaterite from solutions. In the multistep transformation pathway, ACC particles formed, then reduced in size before transforming into aragonite or vaterite. The secondary phase then grew by consuming the initially formed amorphous particles. Nucleation of calcite rhombohedra and hemispherical particles of either ACC or vaterite was detected, together with the nucleation of multiple phases, which was followed by the transformation to secondary phases. In the latter case, vateritic-like crystals along with aragonitic-like particles formed, followed by the nucleation and growth of a calcite rhombohedron as the aragonitic particles dissolved. Finally, ACC particles dissolved either uniformly until complete disappearance, or in a way that left the particles rough and with pits over time, or a combination of the two. This observation suggests that the ACC could have a variety of structures including dense liquid phase and hydrous and anhydrous forms instead of a single or a few closely related structures, and the direct transformation from ACC to calcite is highly unlikely.

In Situ LTEM Study of Oxidative Etching. Preparation of various nanostructures of metallic nanocrystals has been achieved through oxidative etching. This etching process are used to retard reduction rate of precursors,[52,53] to reconstruct as-formed metallic nanocrystals,[54,55] and to generate single crystalline nanocrystals through the removal of highly reactive forms with twin defects or stacking faults.[56] In this regard, in situ LTEM was used to elucidate many details in the oxidative etching processes, such as ion-promoted etching of palladium (Pd) cubic nanocrystals.[57] Figure 5 shows the transformation of a Pd nanocrystal from well-defined cubic to spherical shape. The reduction in size started from the apexes and edges of the nanocube. For isolated particles, the dissolution rate, dr/dt, was found to increase as the size of the nanocrystal decreased, that is, $dr/dt \sim 1/r$. As the nanocrystal became smaller and rounder, chemical potential increased with increasing local curvature, resulting in a faster dissolution rate. For aggregated particles, the dissolution rate was dramatically reduced due to steric hindrance, though overall dissolution dynamics remained similar to those of isolated particles. In situ LTEM study shows the presence of Br^- ions was important and dissolution of Pd nanocrystals was not observed without Br^- ions. When Br^- ions were replaced with Cl^- ions, oxidative etching did not occur, possibly because $[PdCl_4]^{2-}$ ion, which is the likely product formed between Cl^- with Pd^{2+} ions, is 10^{13} times less stable than the $[PdBr_4]^{2-}$ ion.

This study also shows electron beam irradiation played a role in oxidative etching. Without the irradiation of electron beam, Pd nanocrystals remained unchanged even in the presence of Br^- ions. In addition, increasing electron dosage resulted in higher dissolution rates of Pd nanocrystals. These observations indicate that the oxidizing species resulted from electron radiolysis likely participated in the etching process. Nevertheless, the in situ LTEM study offers a close look at the details of the oxidative etching process, which should contribute to the new design principles of nanostructures.

In Situ LTEM Study of the Formation of Nanostructures in a Liquid Flow Cell. Although a static liquid cell can be used to obtain many details on the nucleation and growth, the fluid flow cell technology offers additional advantages for LTEM studies. When a static liquid cell is used, growth solution containing all reaction ingredients and solvents for the synthesis need to be added all together prior to imaging. Initial nucleation events may occur prior to the cell being loaded to the chamber and cannot be recorded. Continuous irradiation of liquid mixtures by an electron beam also lead to unwanted side reactions.[58] In fact, under high dose levels of electron beam, kinetically controlled dendritic growth is often observed and overshadows the processes that one intends to study. Liquid flow cell coupled with low electron dose imaging conditions can be used to address the aforementioned problems. For instance, a liquid flow cell was successfully used to study the details of seed-mediated nucleation and growth, because seeds were separated from the precursor solution from the onset and the dendritic growth due to electron beam was greatly suppressed in the fresh growth media.[28] Continuous fluid flow also helps to remove the products from radiolysis, such as solvated electrons and excess heat, and thus minimizes undesirable, side reactions.[22,59]

The in situ study using liquid flow cell reveals a hybrid nucleation and growth process in 3D nanostructures that had not yet been observed in detail, which involves nucleation-initial island growth, surface diffusion, and subsequent layer-by-layer growth.

Liquid flow cell was used initially to study the formation of lead sulfide (PbS) nanoparticles in a TEM equipped with electron and laser irradiation sources.[59] Solution concentration was shown to affect the rate of reaction, whereas change in composition led to the growth of nanoparticles with different size and shape. Recently, Yang and Zuo groups used liquid flow cell to quantitatively investigate the growth of Au on well-defined icosahedral Pt nanoparticles.[28] By coupling with a low electron dose imaging technique, such a liquid environment represents a step closer to mimicking real synthetic conditions. The in situ study using liquid flow cell reveals a hybrid nucleation and growth process in 3D nanostructures that had not yet been observed in detail, which involves nucleation-initial island growth, surface diffusion, and subsequent layer-by-layer growth, as shown in Figure 6. One important observation was the diffusion of Au atoms to flat facets of the Pt icosahedron began after their initial nucleation and growth at the corner regions. The in situ LTEM shows the distances between two opposite corners or sides did not always increase monotonically but could be in an oscillating fashion, indicating the existence of competing processes. A surface-reaction controlled growth could be confirmed unambiguously based on the quantitative analysis of the in situ data using the LSW theory, which takes reaction and diffusion into account (Figure

DOI: 10.1021/acs.jpclett.5b02210
J. Phys. Chem. Lett. 2015, 6, 5051−5061

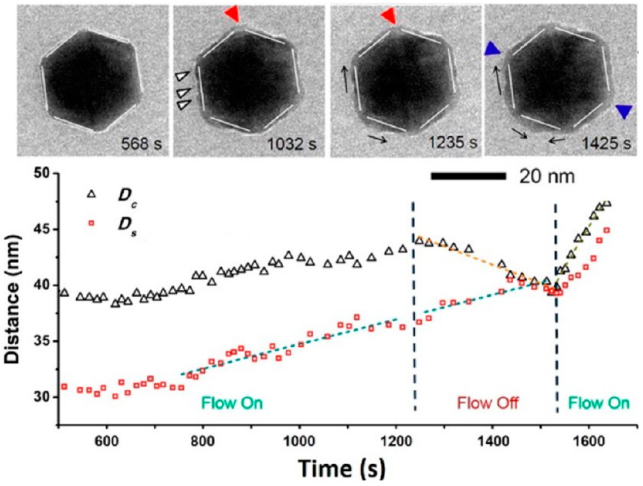

Figure 6. Quantitative in situ LTEM study of the growth of Au on Pt icosahedral nanoparticles using a liquid flow cell. Image is reprinted with permission from ref 28. Copyright 2015 American Chemical Society.

6). In the treatment, the growth rate, dr/dt, can be described by the following equation:[60]

$$\frac{dr}{dt} = \frac{2\sigma V_m^2 c_\infty}{RT[(1/D) + (1/(k_d r))]}\left(\frac{(1/r_b) - (1/r)}{r}\right) \quad (1)$$

where r is the radius, r_b is the critical radius, σ is the interfacial energy between metal and water, c_∞ is the concentration of a monomer in the bulk, V_m is the molar volume, D is the diffusion coefficient, k_d is the rate constant for the deposition, and R is the gas constant. When the reaction is diffusion-limited, the growth rate is dominated by the diffusion of atoms to the surface, that is, $D \ll k_b r$, and eq 1 reduces to

$$\frac{dr}{dt} = \frac{2\sigma D V_m^2 c_\infty}{RT}\left(\frac{(r/r_b) - 1}{r^2}\right) = K_D\left(\frac{(r/r_b) - 1}{r^2}\right) \quad (2)$$

where K_D is a constant. The LSW theory shows that the ratio r/r_b is a constant if the total mass of the system is conserved, leading to the following simplification of eq 2 to the form

$$\frac{dr}{dt} = \frac{K_D(\text{constant})}{r^2} \quad (3)$$

Equation 3 can be solved to obtain the simple relationship between particle size and reaction time

$$r^3 - r_0^3 = Kt, \qquad K = \frac{8\sigma D V_m^2 c_\infty}{9RT} \quad (4)$$

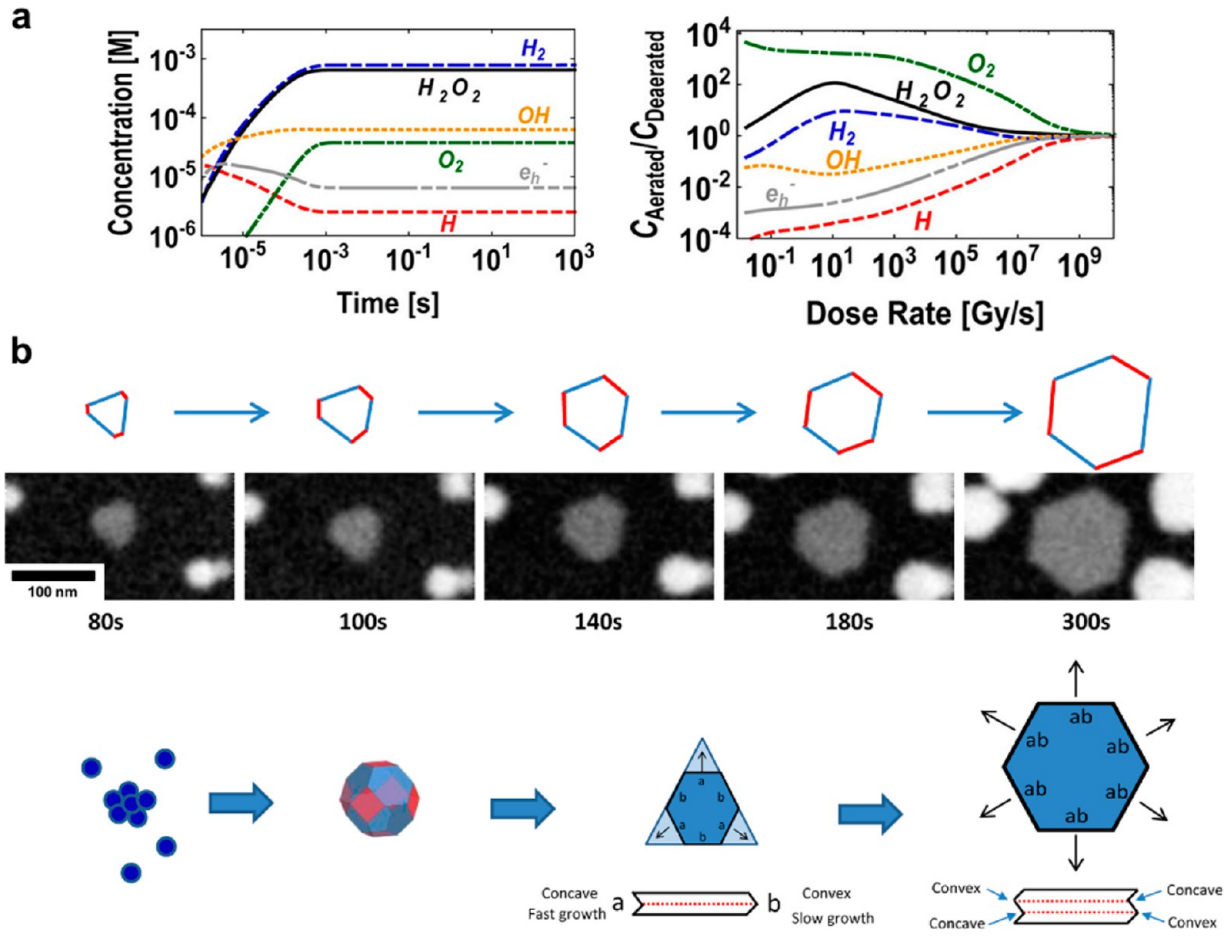

Figure 7. (a) Computed concentration profiles of radiolysis products as functions of time and dose rate. Image is reprinted with permission from ref 62. Copyright 2014 American Chemical Society. (b) Growth of Au nanocrystals using electron beam in LTEM. Image is reprinted with permission from ref 61. Copyright 2015 American Chemical Society.

DOI: 10.1021/acs.jpclett.5b02210
J. Phys. Chem. Lett. 2015, 6, 5051−5061

where r_0 is the initial radius of the particle. When the growth rate is limited by the surface reaction of the monomers, that is, $D \gg k_b r$, eq 1 can be solved in a way similar to the diffusion-limited case to yield the following equation:

$$r^2 \approx K_R t, \qquad K_R = \frac{2\sigma D V_m^2 c_\infty}{RT} \tag{5}$$

Fitting experimental data with theoretical values calculated using eqs 4 and 5 indicated that the growth rate was dominated by surface reaction. The surface diffusion constant was also obtainable based on the in situ LTEM data.

Effect of Electron Beam on the Formation of Nanoparticles Using In Situ LTEM. In an in situ LTEM study, effects of electron beam are unavoidable and sometimes used intentionally in the preparation of nanostructures, although interactions between electron beam and liquid samples often need to be minimized to make sure nanoparticle nucleation and growth take place under typical conditions.[28,58] Most of the LTEM studies take place with a constant electron beam at low dosage current in order to limit electron-induced reactions. Wu et al. performed a control experiment and found that beam induced dendritic growth of Au was not readily observable at an electron dose of 30 electrons/(Å^2·s) under fluid flow conditions.[28] At the same time, electron beam has been used to make metal nanoparticles from the metal precursors.[61,62] A kinetic model was recently developed to simulate the concentration profile of various radiolytic products as a function of irradiation time and dose (Figure 7a).[62] When the entire liquid was homogeneously irradiated, concentration of radiolytic species such as solvated electron, H_2O_2, and OH^- increased monotonically with time and reached steady state within 1 ms after the start of irradiation. In the case of nonuniform irradiation, in which only a fraction of the liquid medium was irradiated, it took seconds for the radiolytic products to reach equilibrium. This is because the radiolytic species that were generated within the irradiated region diffused outward and continued to interact during the process. At the low dose rate, there are different concentration profiles for radiolytic species between the aerated and deaerated aqueous solutions (Figure 7a). In the presence of oxygen, concentrations of radical species such as $HO^\bullet$ and $H^\bullet$ were reduced during the irradiation, whereas those of molecular species such as H_2, H_2O_2, and O_2 increased. Concentrations of all radiolytic species were independent of initial oxygen concentration when they reached the steady state, (Figure 7a). Both growth and etching of gold Au nanorods could occur, because the ratio of concentration between reducing and oxidizing species changed with various dose rates.[62]

Electron beam current in LTEM may be correlated to the concentration of reducing agent in conventional synthesis. An induction threshold of 0.5 electrons/(Å^2·s) was identified for the formation of Ag nanoparticles by electron beam irradiation in a liquid static cell.[63] At a beam current close to the threshold, growth of Ag nanoparticles was limited by the surface reduction reaction, leading to the formation of faceted nanocrystals such as nanoplates. At a beam current ~7 times higher than the threshold, the growth was limited by diffusion, resulting in the formation of spherical nanoparticles. The effects of electron beam on the growth and faceting of Au planar and 3D nanoparticles was also studied using in situ LTEM.[61] Electron dose rate was found to have an effect similar to the concentration of a reducing agent in aqueous synthesis. Low dose conditions led to surface reaction-limited growth, whereas high dose conditions resulted in diffusion-limited growth. More importantly, LTEM data show that in order to form nanoplates and well-faceted 3D nanoparticles, the rate of deposition needs be less than three atomic layers per second.[61] Such a supply rate of metal precursors was measured directly for the formation of faceted nanoparticles. In addition, the role of twin plane in the formation of facets were also explored using in situ LTEM.[61] Figure 7b presents the irreversible transition of Au nanoplates from triangular to hexagonal shapes. This shape transition was thought to originate from the formation of additional twin planes in a growing single-twin nanoprism. When the first twin plane, indicated by the red dashed line in Figure 7b, formed parallel to the top and bottom (111) surfaces, alternating concave and convex structures appeared, resulting in a different growth rate between these two types of edges and the formation of triangular prism. With the appearance of additional twin plane, all sides had both concave and convex structure, and thus a growth in all six side directions to form a hexagon. Parallel (111) twin planes were crucial in the growth and facet formation of 2D nanostructures because monomers preferred to react along selected edges of twin planes.

Summary and Future Outlook. The wealth of details offered by in situ LTEM has turned it into a powerful tool for studying the formation of nanoparticles in liquid and allowed to reveal many never-before-seen insights of the nucleation and growth processes. Design of the liquid cells for LTEM are improving rapidly in many ways, resulting in new capabilities. There are recent developments aimed at reducing the thickness of window[64] and liquid layer,[65] as well as methods to either mitigate electron damage[58] or to use electron beam in the synthesis.[61,63]

There are interesting problems that lie ahead, including the improvement of image resolution and minimization of electron beam-induced effects. Continuous optimizations of liquid cells are often essential in order to better control and understand the conditions during an in situ study. On the design of liquid cell, minimization of window bowing due to pressure difference and reduction in window thickness may greatly improve imaging resolution. Fabrication of nanocolumns bridging the two windows together in a monolithic fashion may minimize the issue of window bowing. The replacement of silicon nitride by graphene has helped to reduce the thickness of window greatly, as graphene is both strong and thin, ideal for constructing a liquid cell.

Resolution can also be improved with the development of faster and more sensitive electron detectors that are capable of imaging robustly at submillisecond frame rates. Such a detector should bring about faster imaging speed to help capture important kinetic details of individual nucleation and growth events, thus greater capability in quantitative analysis. In addition to improving liquid cells, there is a clear need to develop the capability that enables the use of in situ LTEM results to guide the design and preparation of nanoparticles with high level of control over structure, shape, and composition. Further understanding of the electron beam effect is thus necessary.

It is clear though that with the rapid development of liquid cell technology, LTEM has brought about numerous new research opportunities for understanding the fundamental phenomena of nucleation and growth of nanostructures with much-needed in situ data for quantitative analysis. We envision LTEM can become the go-to technique for quantitative study

DOI: 10.1021/acs.jpclett.5b02210
J. Phys. Chem. Lett. 2015, 6, 5051−5061

LTEM has brought about numerous new research opportunities for understanding the fundamental phenomena of nucleation and growth of nanostructures with much-needed in situ data for quantitative analysis.

of various phenomena at true nanoscale in solution, including the new 3D imaging capability[66] and for self-assembly of nanostructures.[67] One may also anticipate the development of new liquid cell technology based on other cues to stimulate growth of nanostructures, such as temperature and electrical biasing. Although greater understanding on the effect of electron-solution interaction is still needed in order to develop the knowledge base for guiding the design and preparation of nanostructures under practical synthetic conditions, there is little doubt that LTEM will enable new and exciting discoveries and, in turn, the development of methods for even greater control over the synthesis of various nanostructures with a high level of precision.

AUTHOR INFORMATION

Corresponding Author

*E-mail: hy66@illinois.edu.

Notes

The authors declare no competing financial interest.

Biographies

Thao Ngo is a Ph.D. student in Chemical and Biomolecular Engineering working in Professor Hong Yang's group at the University of Illinois at Urbana−Champaign. She received her B.S. (2013) in Chemical Engineering from Arizona State University. Her research focuses on using LTEM to understand nanoscale phenomena in solution and degradation mechanism and kinetics of electrocatalysts to improve performance, durability, and stability.

Hong Yang is the Richard C. Alkire Professor in Chemical Engineering at the University of Illinois at Urbana−Champaign. He obtained his Ph.D. degree in 1998 from University of Toronto and did his postdoctoral research at Harvard University. His current research interests include understanding the formation of nanocrystals, catalysis and electrocatalysis, in situ characterization techniques, and nanomaterials for energy and biomedical applications. http://www.scs.illinois.edu/hyang/

ACKNOWLEDGMENTS

We thank U.S. National Science Foundation (CHE-1213926, OISE-1515376) and UIUC for financial supports of this research. The in situ work at UIUC was accomplished through the collaboration with Prof. Jian-Min Zuo group. T.N. is grateful for a NSF Graduate Research Fellowship.

REFERENCES

(1) Ruska, E. The Development of the Electron Microscope and of Electron Microscopy (Nobel Lecture). *Angew. Chem., Int. Ed. Engl.* **1987**, *26*, 595−605.

(2) Lohse, S. E.; Burrows, N. D.; Scarabelli, L.; Liz-Marzan, L.; Murphy, C. J. Anisotropic Noble Metal Nanocrystal Growth: The Role of Halides. *Chem. Mater.* **2014**, *26*, 34−43.

(3) Peng, Z.; You, H.; Yang, H. Composition-Dependent Formation of Platinum Silver Nanowires. *ACS Nano* **2010**, *4*, 1501−1510.

(4) Peng, Z. M.; Yang, H. Designer Platinum Nanoparticles: Shape, Composition in Alloys, Nanostructure and Electrocatalytic Property. *Nano Today* **2009**, *4*, 143−164.

(5) Ruska, E. Beitrag Zur Ubermikroskopischen Abbildung Bei Höheren Drucken. *Colloid Polym. Sci.* **1942**, *100*, 212−219.

(6) Abrams, I. M.; McBain, J. W. A Closed Cell for Electron Microscopy. *Science* **1944**, *100*, 273−274.

(7) Williamson, M. J.; Tromp, R. M.; Vereecken, P. M.; Hull, R.; Ross, F. M. Dynamic Microscopy of Nanoscale Cluster Growth at the Solid-Liquid Interface. *Nat. Mater.* **2003**, *2*, 532−536.

(8) Nielsen, M. H.; Aloni, S.; De Yoreo, J. J. In Situ Tem Imaging of $CaCO_3$ Nucleation Reveals Coexistence of Direct and Indirect Pathways. *Science* **2014**, *345*, 1158−1162.

(9) Smeets, P. J. M.; Cho, K. R.; Kempen, R. G. E.; Sommerdijk, N. A. J. M.; De Yoreo, J. J. Calcium Carbonate Nucleation Driven by Ion Binding in a Biomimetic Matrix Revealed by In Situ Electron Microscopy. *Nat. Mater.* **2015**, *14*, 394−399.

(10) Gu, M.; Parent, L. R.; Mehdi, B. L.; Unocic, R. R.; McDowell, M. T.; Sacci, R. L.; Xu, W.; Connell, J. G.; Xu, P.; Abellan, P.; et al. Demonstration of an Electrochemical Liquid Cell for Operando Transmission Electron Microscopy Observation of the Lithiation/Delithiation Behavior of Si Nanowire Battery Anodes. *Nano Lett.* **2013**, *13*, 6106−6112.

(11) Abellan, P.; Mehdi, B. L.; Parent, L. R.; Gu, M.; Park, C.; Xu, W.; Zhang, Y.; Arslan, I.; Zhang, J. G.; Wang, C. M.; Evans, J. E.; Browning, N. D. Probing the Degradation Mechanisms in Electrolyte Solutions for Li-Ion Batteries by In Situ Transmission Electron Microscopy. *Nano Lett.* **2014**, *14*, 1293−1299.

(12) Thiberge, S.; Nechushtan, A.; Sprinzak, D.; Gileadi, O.; Behar, V.; Zik, O.; Chowers, Y.; Michaeli, S.; Schlessinger, J.; Moses, E. Scanning Electron Microscopy of Cells and Tissues under Fully Hydrated Conditions. *Proc. Natl. Acad. Sci. U. S. A.* **2004**, *101*, 3346−3351.

(13) de Jonge, N.; Ross, F. M. Electron Microscopy of Specimens in Liquid. *Nat. Nanotechnol.* **2011**, *6*, 695−704.

(14) Daulton, T. L.; Little, B. J.; Lowe, K.; Jones-Meehan, J. In Situ Environmental Cell-Transmission Electron Microscopy Study of Microbial Reduction of Chromium(VI) Using Electron Energy Loss Spectroscopy. *Microsc. Microanal.* **2001**, *7*, 470−485.

(15) Mohanty, N.; Fahrenholtz, M.; Nagaraja, A.; Boyle, D.; Berry, V. Impermeable Graphenic Encasement of Bacteria. *Nano Lett.* **2011**, *11*, 1270−1275.

(16) Zheng, H.; Smith, R. K.; Jun, Y. W.; Kisielowski, C.; Dahmen, U.; Alivisatos, A. P. Observation of Single Colloidal Platinum Nanocrystal Growth Trajectories. *Science* **2009**, *324*, 1309−1312.

(17) Liao, H.-G.; Zherebetskyy, D.; Xin, H.; Czarnik, C.; Ercius, P.; Elmlund, H.; Pan, M.; Wang, L.-W.; Zheng, H. Facet Development During Platinum Nanocube Growth. *Science* **2014**, *345*, 916−919.

(18) De Clercq, A.; Dachraoui, W.; Margeat, O.; Pelzer, K.; Henry, C. R.; Giorgio, S. Growth of Pt−Pd Nanoparticles Studied In Situ by HRTEM in a Liquid Cell. *J. Phys. Chem. Lett.* **2014**, *5*, 2126−2130.

(19) Jungjohann, K. L.; Bliznakov, S.; Sutter, P. W.; Stach, E. A.; Sutter, E. A. In Situ Liquid Cell Electron Microscopy of the Solution Growth of Au−Pd Core−Shell Nanostructures. *Nano Lett.* **2013**, *13*, 2964−2970.

(20) Yuk, J. M.; Park, J.; Ercius, P.; Kim, K.; Hellebusch, D. J.; Crommie, M. F.; Lee, J. Y.; Zettl, A.; Alivisatos, A. P. High-Resolution EM of Colloidal Nanocrystal Growth Using Graphene Liquid Cells. *Science* **2012**, *336*, 61−64.

(21) Xin, H. L.; Zheng, H. In Situ Observation of Oscillatory Growth of Bismuth Nanoparticles. *Nano Lett.* **2012**, *12*, 1470−1474.

(22) Ring, E. A.; de Jonge, N. Microfluidic System for Transmission Electron Microscopy. *Microsc. Microanal.* **2010**, *16*, 622−629.

(23) Lamer, V. K.; Dinegar, R. H. Theory, Production and Mechanism of Formation of Monodispersed Hydrosols. *J. Am. Chem. Soc.* **1950**, *72*, 4847−4854.

(24) La Mer, V. K. Nucleation in Phase Transitions. *Ind. Eng. Chem.* **1952**, *44*, 1270−1277.

DOI: 10.1021/acs.jpclett.5b02210
J. Phys. Chem. Lett. 2015, 6, 5051−5061

(25) Lifshitz, I. M.; Slyozov, V. V. The Kinetics of Precipitation from Supersaturated Solid Solutions. *J. Phys. Chem. Solids* **1961**, *19*, 35−50.
(26) Wagner, C. Theorie Der Alterung Von Niederschlagen Durch Umlosen (Ostwald-Reifung). *Z. Elektrochem.* **1961**, *65*, 581−591.
(27) Li, D.; Nielsen, M. H.; Lee, J. R. I.; Frandsen, C.; Banfield, J. F.; De Yoreo, J. J. Direction-Specific Interactions Control Crystal Growth by Oriented Attachment. *Science* **2012**, *336*, 1014−1018.
(28) Wu, J.; Gao, W.; Wen, J.; Miller, D. J.; Lu, P.; Zuo, J.-M.; Yang, H. Growth of Au on Pt Icosahedral Nanoparticles Revealed by Low-Dose In Situ TEM. *Nano Lett.* **2015**, *15*, 2711−2715.
(29) Nair, R. R.; Blake, P.; Blake, J. R.; Zan, R.; Anissimova, S.; Bangert, U.; Golovanov, A. P.; Morozov, S. V.; Geim, A. K.; Novoselov, K. S.; Latychevskaia, T. Graphene as a Transparent Conductive Support for Studying Biological Molecules by Transmission Electron Microscopy. *Appl. Phys. Lett.* **2010**, *97*, 153102.
(30) Erni, R.; Rossell, M. D.; Nguyen, M.-T.; Blankenburg, S.; Passerone, D. Stability and Dynamics of Small Molecules Trapped on Graphene. *Phys. Rev. B: Condens. Matter Mater. Phys.* **2010**, *82*, 165443.
(31) Lee, C.; Wei, X.; Kysar, J. W.; Hone, J. Measurement of the Elastic Properties and Intrinsic Strength of Monolayer Graphene. *Science* **2008**, *321*, 385−388.
(32) Meyer, J. C.; Girit, C. O.; Crommie, M. F.; Zettl, A. Imaging and Dynamics of Light Atoms and Molecules on Graphene. *Nature* **2008**, *454*, 319−322.
(33) Balandin, A. A.; Ghosh, S.; Bao, W.; Calizo, I.; Teweldebrhan, D.; Miao, F.; Lau, C. N. Superior Thermal Conductivity of Single-Layer Graphene. *Nano Lett.* **2008**, *8*, 902−907.
(34) Penn, R. L.; Banfield, J. F. Imperfect Oriented Attachment: Dislocation Generation in Defect-Free Nanocrystals. *Science* **1998**, *281*, 969−971.
(35) Niederberger, M.; Coelfen, H. Oriented Attachment and Mesocrystals: Non-Classical Crystallization Mechanism Based on Nanoparticle Assembly Attachment and Mesocrystals: Non-Classical Crystallization Mechanisms Based on Nanoparticle Assembly. *Phys. Chem. Chem. Phys.* **2006**, *8*, 3271−3287.
(36) Pacholski, C.; Kornowski, A.; Weller, H. Self-Assembly of ZnO: From Nanodots to Nanorods. *Angew. Chem., Int. Ed.* **2002**, *41*, 1188−1191.
(37) Zitoun, D.; Pinna, N.; Frolet, N.; Belin, C. Single Crystal Manganese Oxide Multipods by Oriented Attachment. *J. Am. Chem. Soc.* **2005**, *127*, 15034−15035.
(38) Yamauchi, Y.; Momma, T.; Fuziwara, M.; Nair, S. S.; Ohsuna, T.; Terasaki, O.; Osaka, T.; Kuroda, K. Unique Microstructure of Mesoporous Pt (H(I)-Pt) Prepared via Direct Physical Casting in Lyotropic Liquid Crystalline Media. *Chem. Mater.* **2005**, *17*, 6342−6348.
(39) Liu, B.; Zeng, H. C. Mesoscale Organization of CuO Nanoribbons: Formation of "Dandelions". *J. Am. Chem. Soc.* **2004**, *126*, 8124−8125.
(40) He, T.; Chen, D. R.; Jiao, X. L. Controlled Synthesis of Co_3O_4 Nanoparticles through Oriented Aggregation. *Chem. Mater.* **2004**, *16*, 737−743.
(41) Si, R.; Zhang, Y. W.; You, L. P.; Yan, C. H. Self-Organized Monolayer of Nanosized Ceria Colloids Stabilized by Poly(Vinylpyrrolidone). *J. Phys. Chem. B* **2006**, *110*, 5994−6000.
(42) Giersig, M.; Pastoriza-Santos, I.; Liz-Marzan, L. M. Evidence of an Aggregative Mechanism During the Formation of Silver Nanowires in N,N-Dimethylformamide. *J. Mater. Chem.* **2004**, *14*, 607−610.
(43) Liao, H. G.; Cui, L.; Whitelam, S.; Zheng, H. Real-Time Imaging of Pt_3Fe Nanorod Growth in Solution. *Science* **2012**, *336*, 1011−1014.
(44) Wu, J.; Yang, H. Platinum-Based Oxygen Reduction Electrocatalysts. *Acc. Chem. Res.* **2013**, *46*, 1848−1857.
(45) Finney, E. E.; Finke, R. G. The Four-Step, Double-Autocatalytic Mechanism for Transition-Metal Nanocluster Nucleation, Growth, and Then Agglomeration: Metal, Ligand, Concentration, Temperature, and Solvent Dependency Studies. *Chem. Mater.* **2008**, *20*, 1956−1970.
(46) Liao, H.-G.; Zheng, H. Liquid Cell Transmission Electron Microscopy Study of Platinum Iron Nanocrystal Growth and Shape Evolution. *J. Am. Chem. Soc.* **2013**, *135*, 5038−5043.
(47) Wolf, S. E.; Leiterer, J.; Kappl, M.; Emmerling, F.; Tremel, W. Early Homogenous Amorphous Precursor Stages of Calcium Carbonate and Subsequent Crystal Growth in Levitated Droplets. *J. Am. Chem. Soc.* **2008**, *130*, 12342−12347.
(48) Bewernitz, M. A.; Gebauer, D.; Long, J.; Coelfen, H.; Gower, L. B. A Metastable Liquid Precursor Phase of Calcium Carbonate and Its Interactions with Polyaspartate. *Faraday Discuss.* **2012**, *159*, 291−312.
(49) Wallace, A. F.; Hedges, L. O.; Fernandez-Martinez, A.; Raiteri, P.; Gale, J. D.; Waychunas, G. A.; Whitelam, S.; Banfield, J. F.; De Yoreo, J. J. Microscopic Evidence for Liquid-Liquid Separation in Supersaturated $CaCO_3$ Solutions. *Science* **2013**, *341*, 885−889.
(50) Gebauer, D.; Voelkel, A.; Coelfen, H. Stable Prenucleation Calcium Carbonate Clusters. *Science* **2008**, *322*, 1819−1822.
(51) Van Driessche, A. E. S.; Benning, L. G.; Rodriguez-Blanco, J. D.; Ossorio, M.; Bots, P.; Garcia-Ruiz, J. M. The Role and Implications of Bassanite as a Stable Precursor Phase to Gypsum Precipitation. *Science* **2012**, *336*, 69−72.
(52) Chen, J. Y.; Herricks, T.; Xia, Y. N. Polyol Synthesis of Platinum Nanostructures: Control of Morphology through the Manipulation of Reduction Kinetics. *Angew. Chem., Int. Ed.* **2005**, *44*, 2589−2592.
(53) Chen, J. Y.; Herricks, T.; Geissler, M.; Xia, Y. N. Single-Crystal Nanowires of Platinum Can Be Synthesized by Controlling the Reaction Rate of a Polyol Process. *J. Am. Chem. Soc.* **2004**, *126*, 10854−10855.
(54) Tao, A.; Sinsermsuksakul, P.; Yang, P. Polyhedral Silver Nanocrystals with Distinct Scattering Signatures. *Angew. Chem., Int. Ed.* **2006**, *45*, 4597−4601.
(55) Mulvihill, M. J.; Ling, X. Y.; Henzie, J.; Yang, P. Anisotropic Etching of Silver Nanoparticles for Plasmonic Structures Capable of Single-Particle SERS. *J. Am. Chem. Soc.* **2010**, *132*, 268−274.
(56) Wiley, B. J.; Xiong, Y. J.; Li, Z. Y.; Yin, Y. D.; Xia, Y. N. Right Bipyramids of Silver: A New Shape Derived from Single Twinned Seeds. *Nano Lett.* **2006**, *6*, 765−768.
(57) Jiang, Y.; Zhu, G.; Lin, F.; Zhang, H.; Jin, C.; Yuan, J.; Yang, D.; Zhang, Z. In Situ Study of Oxidative Etching of Palladium Nanocrystals by Liquid Cell Electron Microscopy. *Nano Lett.* **2014**, *14*, 3761−3765.
(58) Woehl, T. J.; Jungjohann, K. L.; Evans, J. E.; Arslan, I.; Ristenpart, W. D.; Browning, N. D. Experimental Procedures to Mitigate Electron Beam Induced Artifacts During In Situ Fluid Imaging of Nanomaterials. *Ultramicroscopy* **2013**, *127*, 53−63.
(59) Evans, J. E.; Jungjohann, K. L.; Browning, N. D.; Arslan, I. Controlled Growth of Nanoparticles from Solution with In Situ Liquid Transmission Electron Microscopy. *Nano Lett.* **2011**, *11*, 2809−2813.
(60) Viswanatha, R.; Sarma, D. D. Growth of Nanocrystals in Solution. In *Nanomaterials Chemistry*; Wiley-VCH: Weinheim, Germany, 2007; pp 139−170.
(61) Alloyeau, D.; Dachraoui, W.; Javed, Y.; Belkahla, H.; Wang, G.; Lecoq, H.; Ammar, S.; Ersen, O.; Wisnet, A.; Gazeau, F.; Ricolleau, C. Unravelling Kinetic and Thermodynamic Effects on the Growth of Gold Nanoplates by Liquid Transmission Electron Microscopy. *Nano Lett.* **2015**, *15*, 2574−2581.
(62) Schneider, N. M.; Norton, M. M.; Mendel, B. J.; Grogan, J. M.; Ross, F. M.; Bau, H. H. Electron−Water Interactions and Implications for Liquid Cell Electron Microscopy. *J. Phys. Chem. C* **2014**, *118*, 22373−22382.
(63) Woehl, T. J.; Evans, J. E.; Arslan, I.; Ristenpart, W. D.; Browning, N. D. Direct In Situ Determination of Mechanisms Controlling Nanoparticle Nucleation and Growth. *ACS Nano* **2012**, *6*, 8599−8610.
(64) Jensen, E.; Burrows, A.; Molhave, K. Monolithic Chip System with a Microfluidic Channel for In Situ Electron Microscopy of Liquids. *Microsc. Microanal.* **2014**, *20*, 445−451.
(65) Grogan, J. M.; Bau, H. H. The Nanoaquarium: A Platform for In Situ Transmission Electron Microscopy in Liquid Media. *J. Microelectromech. Syst.* **2010**, *19*, 885−894.

DOI: 10.1021/acs.jpclett.5b02210
J. Phys. Chem. Lett. 2015, 6, 5051−5061

(66) Park, J.; Elmlund, H.; Ercius, P.; Yuk, J. M.; Limmer, D. T.; Chen, Q.; Kim, K.; Han, S. H.; Weitz, D. A.; Alivisatos, A. P. 3D Structure of Individual Nanocrystals in Solution by Electron Microscopy. *Science* **2015**, *349*, 290−295.
(67) Chen, Q.; Cho, H.; Manthiram, K.; Yoshida, M.; Ye, X.; Alivisatos, A. P. Interaction Potentials of Anisotropic Nanocrystals from the Trajectory Sampling of Particle Motion Using In Situ Liquid Phase Transmission Electron Microscopy. *ACS Cent. Sci.* **2015**, *1*, 33−39.

DOI: 10.1021/acs.jpclett.5b02210
J. Phys. Chem. Lett. 2015, 6, 5051−5061